JOURNAL OF PROTEOMICS 73 (2010) 951–964

available at www.sciencedirect.com

ScienceDirect

www.elsevier.com/locate/jprot

Studies on glyphosate-induced carcinogenicity in mouse skin: A proteomic approach

*Jasmine George, Sahdeo Prasad, Zafar Mahmood, Yogeshwer Shukla**

Proteomics Laboratory, Indian Institute of Toxicology Research (CSIR), Mahatma Gandhi Marg, Lucknow 226001 (U.P.), India

ARTICLE INFO

Article history:
Received 25 September 2009
Accepted 15 December 2009

Keywords:
Glyphosate
TPA
Tumor promotion
Mass spectrometry
Hierarchical cluster analysis
Biomarkers

ABSTRACT

Glyphosate is a widely used broad spectrum herbicide, reported to induce various toxic effects in non-target species, but its carcinogenic potential is still unknown. Here we showed the carcinogenic effects of glyphosate using 2-stage mouse skin carcinogenesis model and proteomic analysis. Carcinogenicity study revealed that glyphosate has tumor promoting activity. Proteomic analysis using 2-dimensional gel electrophoresis and mass spectrometry showed that 22 spots were differentially expressed (>2 fold) on glyphosate, 7, 12-dimethylbenz[a]anthracene (DMBA) and 12-O-tetradecanoyl-phorbol-13-acetate (TPA) application over untreated control. Among them, 9 proteins (translation elongation factor eEF-1 alpha chain, carbonic anhydrase III, annexin II, calcyclin, fab fragment anti-VEGF antibody, peroxiredoxin-2, superoxide dismutase [Cu–Zn], stefin A3, and calgranulin-B) were common and showed similar expression pattern in glyphosate and TPA-treated mouse skin. These proteins are known to be involved in several key processes like apoptosis and growth-inhibition, anti-oxidant responses, etc. The up-regulation of calcyclin, calgranulin-B and down-regulation of superoxide dismutase [Cu–Zn] was further confirmed by immunoblotting, indicating that these proteins can be good candidate biomarkers for skin carcinogenesis induced by glyphosate. Altogether, these results suggested that glyphosate has tumor promoting potential in skin carcinogenesis and its mechanism seems to be similar to TPA.

1. Introduction

Pesticides, used extensively for controlling pest and destroying weeds are ubiquitous contaminants accumulating in environment and hence humans get unavoidably exposed to these pesticides. About 3 billion tons of pesticides are used every year, on agricultural crops worldwide [1]. In some cases, even short-term exposure of the pesticides can make impact on human health. Apart from the other toxic effects, pesticides are reported to cause genotoxicity/carcinogenicity also. Some pesticides have been classified as carcinogens by the United States Environmental Protection Agency (USEPA) [2] and International Agency for Research on Cancer (IARC) [3]. Glyphosate, N-(phosphonomethyl) glycine, commonly sold as a commercial formulation named, Roundup is a widely used herbicide on both cropland and non-cropland areas [4]. The potential activity of glyphosate is through competitive inhibition of the enolpyruvyl-shikimate-phosphate synthase, an enzyme essential to the synthesis of aromatic amino acids in plants [5]. Toxicological profile of glyphosate, showed that it is a comparatively safe herbicide for animals [6]. Glyphosate alone or with its formulation products, such as, surfactants and permeabilizing agents is usually considered to be harmless under both normal usage and chronic exposure [4]. In 1993, USEPA categorized this compound into class E, which means that it is probably not carcinogenic to humans [7]. Despite these reports, some case-control studies suggested an association between glyphosate exposure and the risk of non-

* *Corresponding author*. Tel.: +91 094151 58430; fax: +91 522 2628227.
E-mail addresses: yogeshwer_shukla@hotmail.com, yshukla@iitr.res.in (Y. Shukla).

1874-3919/$ – see front matter © 2009 Elsevier B.V. All rights reserved.
doi:10.1016/j.jprot.2009.12.008

Hodgkin's lymphoma [8,9]. In another study, both technical grade glyphosate and Roundup were shown to cause a rapid increase in cell division in human breast cancer cells [10]. Glyphosate has also been shown as a skin irritant [11]. Regarding the genotoxic potential, glyphosate exposure to human lymphocytes *in vitro* resulted in increased sister chromatid exchanges [12], chromosomal aberrations [13], and indicators of oxidative stress [14]. A recent study from our laboratory also showed the clastogenic effects of glyphosate in bone marrow cells of Swiss albino mice [15]. These reports prompted us to investigate its carcinogenic effect in long-term animal bioassay.

To evaluate toxicity/carcinogenicity induced by physical and chemical agents including pesticides, various test systems have been employed in bacteria, rodents and mammalian cells [16–18]. Each of these environmental challenges causes changes in DNA conformation, alterations in the levels of mRNA and protein expression, and post-translational modifications such as phosphorylation and glycosylation of proteins specific to each stressor [19]. In recent years, there has been considerable interest in linking carcinogenic/toxic responses to gene and protein expression. Toxicoproteomics has received a lot of attention as a valuable tool to search reliable early predictive toxicity markers in response to environmental stimuli [20]. Two-dimensional gel electrophoresis (2-DE) coupled with mass spectrometry (MS); a high-throughput technique allows proteins of interest to be identified by their expression and/or modification pattern rather than using the traditional approach of translating gene expression data. Biomarkers can be used to identify causal associations and to make better quantitative estimates of those associations at relevant levels of exposure [21]. Yamamoto et al. [22] have utilized proteomic approach to identify potential biomarker candidates of hepatotoxicant exposure in rat liver.

Skin is the largest organ in the body and dermal contact is one of the most probable routes of human exposure to pesticides, thus, mouse skin model represents a logical experimental choice [23]. As the long-term bioassay for carcinogenicity is expansive, time consuming and involves a large number of animals and ethical issues, development of biomarkers after short-term exposure are needed. The present investigation was carried out to study the carcinogenic potential of glyphosate and to identify differentially expressed proteins, using 2-DE and MS analysis after treatment with glyphosate, a known tumor promoter, 12-o-tetradecanoylphorbol-13-acetate (TPA) and tumor initiator, 7, 12-dimethylbenz[a]anthracene (DMBA) in mouse skin. Altered proteins identified through proteomic approach in our study may be potentially useful as early biomarkers, to detect the adverse effects of glyphosate.

2. Materials and methods

2.1. Materials

The commercial formulation of the herbicide glyphosate (*N*-phosphonomethyl-glycine) Roundup Original® (glyphosate 41%, POEA≈15%—Monsanto Company, St. Louis, MO, USA) was used, which contains 360 g/l glyphosate acid equivalent as the isopropylamine salt and was procured from local market. Immobilized pH gradient (IPG) strips and 0.5% pH 3–10 IPG buffer were purchased from Bio-Rad Laboratories (Hercules, CA, USA). DMBA, TPA, CHAPS, DTT, and beta-actin (clone AC-74) antibody were from Sigma-Aldrich (Missouri, USA). DNase/RNase was from Bangalore Genei (Bangalore, India). The rest of the chemicals used in the study were of analytical grade of purity and procured locally.

2.2. Animals and treatments

2.2.1. Carcinogenicity study

Male, Swiss albino mice (12–15 g body weight [b.wt]) were taken from Indian Institute of Toxicology Research (IITR) animal breeding colony and acclimatized for 1 week. The ethical approval for the experiment was obtained from institutional ethical committee. The animals were kept under standard laboratory conditions (temperature 23±2 °C, relative humidity 55±5%) and were fed with synthetic pellet basal diet (Ashirwad, Chandigarh, India) and tap water *ad libitum*. Animals were randomly divided into 8 groups of 20 animals each. Hair were clipped in the dorsal region with proper care in an area of 2 cm^2 using electrical clippers, not lubricated with oil or grease. The long-term treatment was given as described earlier [24]. Briefly,

- Group I Untreated control (No treatment).
- Group II Glyphosate alone (25 mg/kg b.wt, topically 3 times per week).
- Group III DMBA+TPA (Single topical application of DMBA, 52 μg/mouse followed 1 week later by thrice a week application of TPA, 5 μg/mouse).
- Group IV Glyphosate (s)+TPA (Single topical application of glyphosate, 25 mg/kg b.wt followed 1 week later by TPA application as in group III).
- Group V Glyphosate (m)+TPA (Thrice a week topical application of glyphosate, 25 mg/kg b.wt for 3 weeks [total of 9 applications], followed 1 week later by TPA application as in group III).
- Group VI DMBA (Single topical application of DMBA, 52 μg/mouse).
- Group VII TPA (Thrice a week topical application of TPA, 5 μg/mouse).
- Group VIII DMBA+glyphosate (Single topical application of DMBA [as in group III], followed 1 week later by topical treatment of glyphosate, 25 mg/kg b.wt thrice per week).

Vehicle for glyphosate, DMBA and TPA were 50% ethanol and acetone respectively.

Animals from all the groups were examined every week for gross morphological changes including body weight changes, development and volume of squamous cell papillomas (tumors) locally on the skin during the entire study period and tumors larger than 1 mm diameter, were included in the total number of tumors. Tumor volume per tumor bearing mouse was calculated in each group using formula $V=D\times d^2\times \pi/6$ (where D=bigger dimension and d=smaller dimension). All the surviving animals were sacrificed at the end of the study period, i.e. 32 weeks for complete carcinogenic, tumor initiating and promoting studies.

2.2.2. Proteomic study

For the proteomic studies, mice of similar sex, age and weight as used for carcinogenicity study were selected. Animals were divided into 4 groups of 4 animals each and treatment was given as described below:

Group I Untreated controls (No treatment).
Group II Glyphosate (Single topical application, 50 mg/kg b. wt/mouse).
Group III DMBA (Single topical application of DMBA, 104 μg/mouse).
Group IV TPA (Single topical application of TPA, 10 μg/mouse).

2.3. Sample preparation for 2-DE

After 24 h, the animals were sacrificed humanly, and skin tissues from the treatment site were excised with the help of sharp scissor and transferred into precooled dishes. The hair were removed with sharp scalpel blades, and subcutaneous fat was scrapped off, on ice. Small pieces of cleaned skin tissues of each mouse from all the groups were then homogenized (10% w/v) individually, in 2-DE lysis buffer containing 8 M urea, 4% CHAPS, 10 mM DTT, 0.5% pH 3–10 IPG buffer, 5 mM TBP, DNase/RNase and 1 mM PMSF. The lysed samples were sonicated for 10 s for 3 strokes followed by a centrifugation at 13,000 rpm for 30 min at 4 °C and pooled for the respective group. After quantification of proteins by Lowry's method, the supernatants were stored at −80 °C until use for electrophoresis.

2.4. 2-DE for differential protein expression

IEF was carried out using commercially dedicated equipment, Protean IEF Cell (Bio-Rad, Hercules, CA, USA). For the first dimension, 17 cm non-linear IPG (pH 3–10) strips were used as per manufacturer's instructions with minor modifications. Briefly, 250 μg of protein from each pooled sample was diluted to 300 μl with rehydration solution (7 M urea, 2 M thiourea, 4% CHAPS, 65 mM DTT, 0.5% pH 3–10 IPG buffer, and trace bromophenol blue), and applied by passive rehydration on separate IPG strips. IEF was performed for each individual sample to a total of 45.5 kVh. All IEF steps were carried out at 20 °C. After the first-dimensional IEF, focused IPG strips were placed in an equilibration solution (6 M urea, 2% SDS, 20% glycerol, 50 mM Tris–HCl, and 0.01% w/v bromophenol blue) containing 1% DTT for 15 min with shaking in the first step followed by 2.5% w/v IAA in equilibration buffer for an additional 15 min in the second step. The gels were then transferred and placed on a 12% polyacrylamide gel and a 0.5% low melting agarose overlay containing 0.1% SDS and 37.5 mM Tris (pH 8.8), was warmed to its melting point and used to seal the IPG strips to the surface of the gel. Molecular weight markers were placed onto the gel by pipetting 8–10 μl onto a piece of blotting paper which was then loaded onto the gel surface. Separation in the second dimension was carried out using Protean II xi electrophoresis equipment (Bio-Rad, Hercules, CA, USA) and Tris–glycine–SDS (pH 8.3) as the electrode buffer, the gels were run at 15 mA/gel until the bromophenol blue dye marker had reached the bottom of the gel. Each experiment was performed in triplicate to obtain the reproducible results.

2.5. Staining and image analysis

After completion of the second-dimension electrophoresis, the gels were fixed and stained by using a fast silver staining protocol with neutral silver nitrate [25]. Analysis of the gels including background subtraction, spot detection, volume normalization and differences in protein expression levels among samples were analyzed by using PDQuest software Ver. 7.4.0 (Bio-Rad Hercules, CA, USA). To determine the variation, 3 gels were prepared for each sample. The protein spots that varied >2 fold change and were specific for the test groups and the control group were manually labeled and considered for MS analysis.

2.6. Matrix-assisted laser desorption/ ionization time-of-flight (MALDI-TOF/TOF) and liquid chromatography mass spectrometry (LC-MS) for protein identification

Differential protein spots of interest were excised manually by using pipette tips and washed 3 times with de-ionized water. Each spot was placed into a 1.5 ml microtube filled with de-ionized water. In-gel digestion for peptide mass fingerprint (PMF) analysis and mass spectrometric analysis were performed at The Centre for Genomic Applications, New Delhi (India). In brief, trypsinized peptide samples were dissolved and mixed with matrix, namely α-cyano-4-hydroxy cinnamic acid. Following drying, the peptides were spotted on ground steel plate and subjected to Bruker Ultraflex MALDI-TOF/TOF and 2D Nano LC-ESI-Trap (Agilent) for mass spectrometric identification. The MALDI-TOF/TOF was equipped with a pulsed nitrogen laser. System calibration was performed using peptide fragment peaks produced by auto-digestion of trypsin as an internal standard for every peptide sample to ensure high mass accuracy and to control possible variations arose due to protein extraction, trypsinization, reconstitution and suppression of ionization by highly abundant species and incomplete/non-homogeneous crystallization of proteins and peptides during matrix preparation.

Data acquisition and analysis was performed using flex control and flex analysis/biotools version 2.2 software, respectively. Data was acquired in reflectron positive mode using 15–18% laser power. Mass tolerance and monoisotopic values (50 ppm/100 ppm for peptide mass fingerprint and peptide mass tolerance of 2 Da for MS/MS spectra) were used for searching. The missed cleavage sites were allowed up to 1; the fixed modification was selected as carbamidomethylation (cysteine); the variable modification was selected as oxidation (methionine). Probability based MOWSE score was calculated in terms of ion score −10 Log (P), where P is the probability and observed match was considered as a random event. Protein scores were derived from ions as a non-probabilistic basis for ranking protein hits and proteins identified by MALDI-TOF and LC/MS were in the expected size range based on its position in the gel. The datasets of the MS spectra, including peptide sequence information, were searched against the SWISS-PROT (GeneBio, Geneva, Switzerland) and NCBInr database using Mascot Daemon (Matrix Science, London, UK) as a client attached to the Mascot search protocol.

2.7. Immunoblot analysis

The differential proteins screened with 2-DE were confirmed by Western blotting. Briefly, skin tissue samples were lysed in lysis buffer (8 M urea, 4% CHAPS, 10 mM DTT, 0.5% pH 3–10 IPG buffer, 5 mM TBP, DNase/RNase and 1 mM PMSF) and resolved on 12–15% polyacrylamide gel, then electro-transferred onto polyvinylidene fluoride membranes (Millipore, USA). After blocking with 5% non-fat dry milk, the membranes were immunoblotted with antibodies of calcyclin (Santa Cruz Biotechnology Inc., Europe), calgranulin-B (Santa Cruz Biotechnology Inc., Europe), superoxide dismutase [Cu–Zn] (SOD 1) (Santa Cruz Biotechnology Inc., Europe) and beta-actin at dilutions recommended by the suppliers. Horse radish conjugated secondary antibodies and chemiluminescence kit (Millipore, USA), were used for detection. Protein expression was visualized by Versa Doc Imaging System (Bio-Rad, Hercules, CA, USA). The intensity was given in terms of relative pixel density for each band normalized to band of beta-actin. The intensity of the bands was measured using software UNSCAN-IT automated digital system version (Orem, USA).

2.8. Statistical analysis

The skin tumor incidence was analyzed by one-way analysis of variance (ANOVA) test in untreated control and treated groups, $p<0.05$ value was considered as significant. Protein expression data for untreated control and treated groups are expressed as the mean ± SD of 3 replicate gels for fold changes of normalized spot volumes. For the statistical analysis of data, Student-t-test was used and $p<0.05$ was considered as significant. Hierarchical clustering analysis using Ward's minimum variance was performed by NCSS software (Kaysville, Utah, USA).

3. Results

3.1. Carcinogenic potential of glyphosate

Carcinogenic potential of glyphosate was recorded in 2-stage mouse skin tumor initiation–promotion protocol when tested as a tumor promoter, however, glyphosate exposure failed to provoke neoplastic development when tested as tumor initiator or complete carcinogen. In this study, conducted to evaluate tumor promoting potential of glyphosate, onset of tumorigenesis was recorded in the animals of positive control group III i.e. DMBA + TPA after 52 days of promotion. All the animals of this group attained tumorigenesis by the end of 112 days of promotion. However, tumor development started in the animals of group VIII (DMBA + glyphosate) after 130 days of promotion and at the time of termination of experiment i.e. 32 weeks, 40% of the animals developed tumors on the dorsal region of the skin (Fig. 1A, Table 1). The total number of tumors in group III was 156 while in group VIII it was 23. No tumor development was observed in the animals of groups I, II, VI and VII during the entire period of study. Similarly, the average

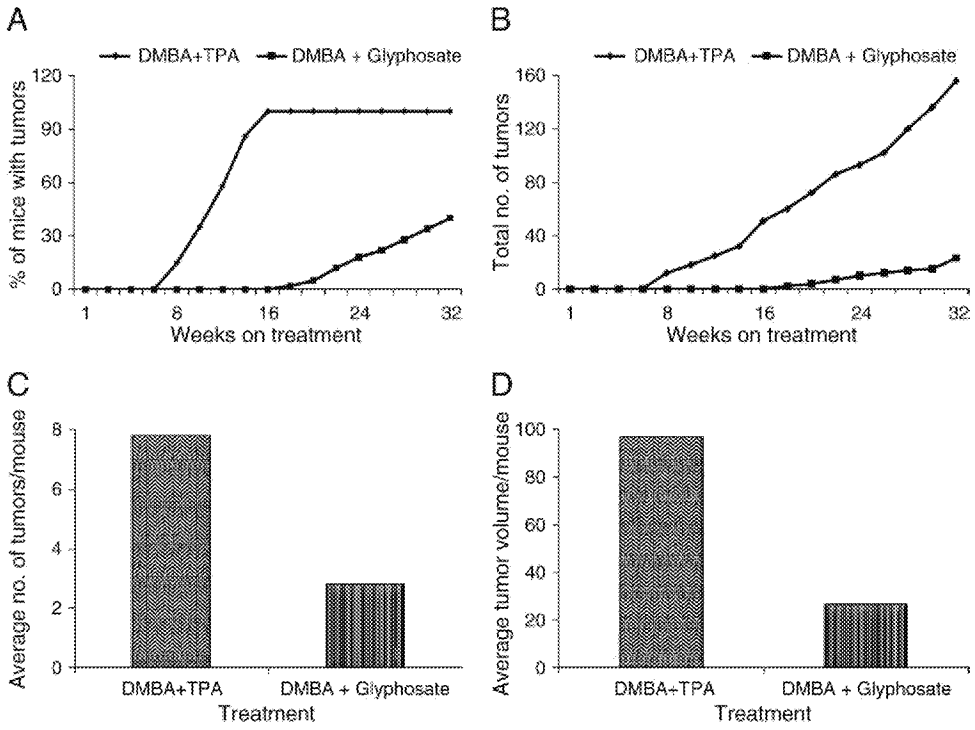

Fig. 1 – Tumor promoting effect of glyphosate in 2-stage mouse skin model of carcinogenesis. Tumor data is represented as (A) y-axis showing the percentage of mice with tumors and x-axis showing the weeks of treatment; (B) y-axis showing the total number of tumors and x-axis showing the weeks of treatment; (C) y-axis showing the average no. of tumors/mouse and x-axis showing the treatment; (D) y-axis showing the average volume of tumors per mouse (mm^3) and x-axis showing the treatment. The values obtained in (C) and (D) are encountered at the end point of study duration i.e. 32 weeks.

Table 1 – Role of carcinogenic, tumor initiating and tumor promoting effect of glyphosate in mouse skin model of carcinogenesis.

Groups	Treatment	Number of animals with tumors	1st induction of tumor (in days)	% of animals with tumors	Total number of tumors	Avg. no. of tumors/mouse (mean ± SD)	Avg. tumor volume/ tumor bearing mouse (mm^3) (mean ± SD)
I	Untreated	0/20	–	–	–	–	–
II	Glyphosate	0/20	–	–	–	–	–
III	DMBA + TPA*	20/20*	52	100	156	7.8±1.1	96.4±5.1
IV	Glyphosate (s) + TPA	0/20	–	–	–	–	–
V	Glyphosate (m) + TPA	0/20	–	–	–	–	–
VI	DMBA (s)	0/20	–	–	–	–	–
VII	TPA	0/20	–	–	–	–	–
VIII	DMBA + glyphosate	8/20*	130	40	23	2.8±0.9	26.2±4.8

*$p < 0.05$ versus untreated group (ANOVA test). s = single dose, m = multiple dose. Details of treatment are provided in Materials and methods section.

number of tumors was 7.8 ± 1.1 in group III, however, in group VIII, it was 2.8 ± 0.9 (Fig. 1C; Table 1). These tumors were initiated as a minute wart like growth, which progressed during the course of experiment and average tumor volume was 96.4 ± 5.1 mm^3 in group III and 26.2 ± 4.8 mm^3 in group VIII (Fig. 1D; Table 1). These results clearly indicate significant tumor promoting potential of glyphosate in mouse skin model of carcinogenesis.

3.2. *Protein expression profile*

Using 2-DE, comparisons of differentially expressed proteins were made in mouse skin following topical treatment with glyphosate (50 mg/kg b.wt/mouse), TPA (10 μg/mouse) and DMBA (104 μg/mouse) with untreated mouse skin individually, using PDQuest 7.4.0 2-D gel analysis software. Representative 2-DE maps are shown in Fig. 2. Image matching derived from 4 groups showed a total of ~2600 spots. Out of these, 22 spots were differentially expressed, exhibiting >2 fold change between values of treated and control animals (Fig. 2). These spots were excised from the gels and analyzed using MALDI-TOF/TOF mass spectrometer. PMF from the proteins was obtained and the resulting spectra were used to identify the proteins with the Mascot search program. Protein spots that appeared more than once, were considered as the same protein and assigned the same number. These identified proteins were categorized according to their molecular functions (Table 2), biological functions and subcellular localization (Fig. 3A and B) as referred to SWISS-PROT database. Protein spot nos. 7 and 18-1, 18-2 were up-regulated and spot no. 13 was down-regulated by glyphosate and TPA treatment (Fig. 4). Related fingerprint mass spectra of calcyclin, calgranulin-B and SOD 1are shown in Fig. 5.

3.3. *Protein expression profile in glyphosate and TPA-treated mouse skin*

Substantially common and differentially expressed protein spots among glyphosate and TPA-treated skin tissues were quantitatively analyzed individually. Comparison between the gels of glyphosate and TPA revealed that 13 specific proteins spots (1, 2, 3, 6-1, 6-2, 7, 8, 11, 12, 13, 15, 18-1, and 18-2) from a total of 22 spots were showing the similar expression pattern. Among the selected and identified proteins with statistically significant altered expression ($p < 0.05$), we focused on the proteins involved in apoptosis and growth-inhibition, anti-oxidation, energy metabolism, angiogenesis, calcium binding and protein biosynthesis processes. These proteins are translation elongation factor eEF-1 alpha chain (eEF1A1), carbonic anhydrase 3 (CA III), annexin II, calcyclin, fab fragment of anti-VEGF antibody, peroxiredoxin-2 (PRX II), superoxide dismutase [Cu–Zn] (SOD 1), stefin A3 and calgranulin-B (Fig. 6, Table 3).

3.4. *Protein expression profile in glyphosate and DMBA treated mouse skin*

Among the 22 differentially expressed protein spots, 4 specific spots (1, 3, 11, and 12) were showing the similar expression pattern between the gels of glyphosate and DMBA treated skin tissues. These proteins are eEF1A1, CA III, fab fragment of anti-VEGF antibody and PRX II (Fig. 6, Table 3).

3.5. *Cluster analysis of differentially expressed proteins in control, glyphosate, TPA and DMBA treated mouse skin*

To understand the carcinogenic activity of glyphosate in mouse skin based on the level of protein expression information generated on 2-DE gels hierarchical cluster analysis was applied. The analysis facilitated the visualization of groupings based on the protein expression changes, potentially showing the relationship between glyphosate and TPA, which further lends support to their tumor promoting activity. A hierarchical clustering map is generated with the differentially expressed protein spots. The analysis showed 2 major clusters, one cluster includes TPA and glyphosate, where majority of the altered protein expression was recorded and the other cluster includes DMBA and control having comparatively low number of altered proteins (Fig. 7). Moreover, calcyclin and calgranulin-B were present only in the cluster of glyphosate and TPA whereas SOD 1 is higher in DMBA and control cluster in comparison to other cluster.

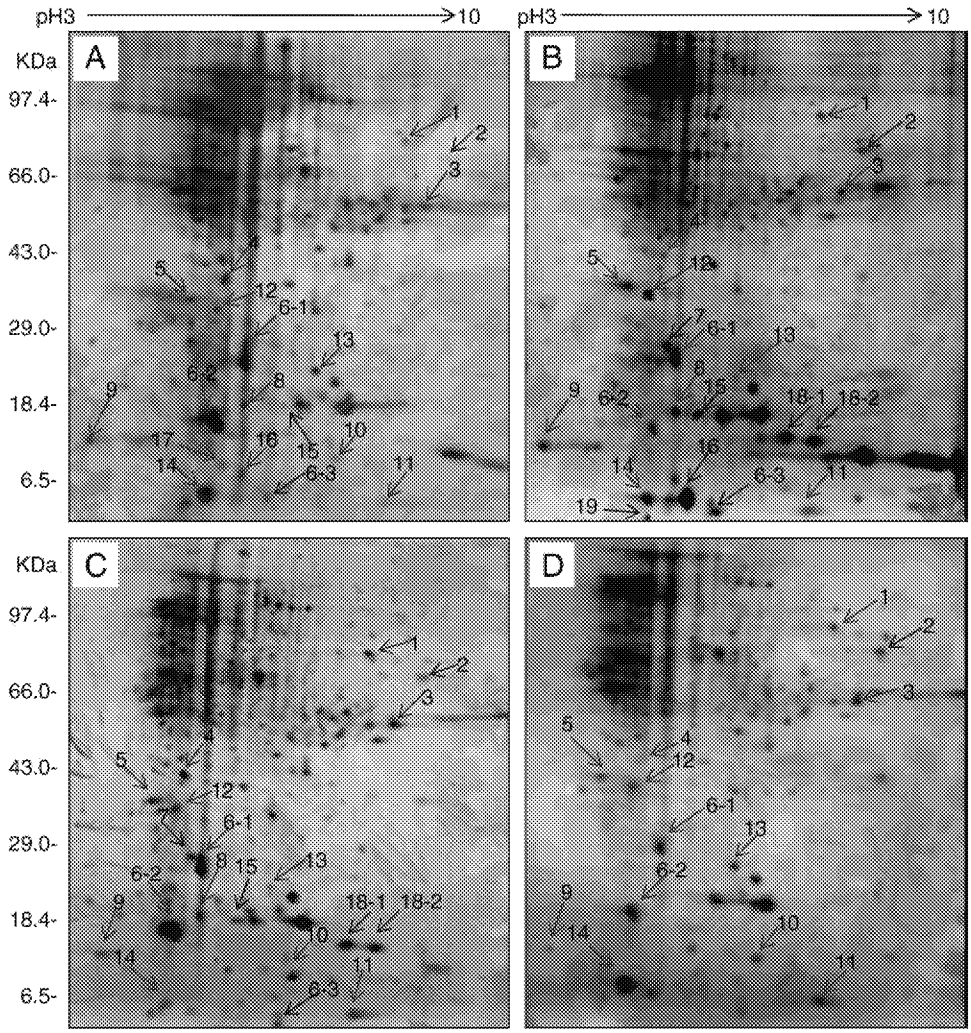

Fig. 2 – Representative 2-DE maps of control and treated groups. A. Untreated control; B. Glyphosate; C. TPA; D. DMBA. The pH gradient is indicated on the top of the gels horizontally, and migration positions of molecular weight markers are indicated on vertical axis. Identified 22 protein spots, selected by quantitative analysis of respective groups are indicated by arrows and labeled as 1 to 19 (details are given in Material and methods section). Repeated spots (albumin and calgranulin-B) identified as same protein are assigned same number.

3.6. *Immunoblot verification of calcyclin, calgranulin-B and SOD 1*

Western blotting showed that the expression of calcyclin and calgranulin-B were significantly increased and that of SOD 1 decreased in the glyphosate and TPA-treated groups only as compared with respective control and DMBA, and the expression patterns of the selected proteins were consistent with the results obtained in 2-DE image analysis (Fig. 8).

4. Discussion

Considering the uses of glyphosate throughout the world, genotoxic/carcinogenic risk associated with its uses needs to be addressed urgently. In the present study, using conventional 2-stage initiation–promotion protocol [24] and proteomic application in animal bioassay for carcinogenicity, we attempted to provide insight into whether glyphosate can induce neoplastic changes.

Results of the animal carcinogenicity bioassay showed that topical application of glyphosate was capable of promoting DMBA-initiated mouse skin cells. However, glyphosate failed to provoke tumorigenesis when tested for initiating and complete carcinogenic activity in mouse skin. The tumor promoting property of glyphosate, as observed in the present study, is in consistency with previous reports, where glyphosate is reported to induce cell proliferation and interfere with cell cycle regulation [26,27]. These results confirmed that glyphosate has tumor promoting activity. Since glyphosate possesses only tumor promoting activity, and not tumor initiating, therefore, it failed to induce tumorigenesis when tested for complete carcinogenic activity.

Mammalian skin cells are continuously exposed to a variety of environmental stresses, each of which may result

Table 2 – Identification of differentially expressed protein spots in treated and control mouse skin by mass spectrometry and database searches.

Spot no.	Protein name/function	Gene	Score	Theory/observed		Accession no.	No. of matched peptides (% sequence coverage)
				[b]Mr (kDa)	[c]pI		
1	Translation elongation factor eEF-1 alpha chain/protein binding, GTP binding	EF-1A	114	50.3/70	9.16/8.9	P10126	5 (8)
2	Ig gamma-2b chain C region/antigen binding	IGHG1	53	45.0/65.0	6.1/8.6	P01867	3 (10)
3	Carbonic anhydrase III/pH balance	CAIII	90	29.5/50	6.97/9.0	P16015	6 (39)
4	[a]NID						
5	Actin gamma/ATP binding, protein binding	ACTG1	98	42.2/40.0	5.31/5.5	P63270	6 (20)
6-1	Albumin (fragment)/protein binding, toxin binding	ALB	146	24.2/28.0	5.48/5.6	P07724	14 (47)
6-2	Albumin (fragment)/protein binding, toxin binding	ALB	108	24.2/17.5	5.48/5.00	P07724	9 (43)
6-3	Albumin (fragment)/protein binding, toxin binding	ALB	61	24.2/24.0	5.48/6.1	P07724	3 (14)
7	Calcyclin/calcium ion binding	S100A6	75	10.1/25	5.3/5.2	P14069	5 (30)
8	Annexin II/calcium ion binding	ANXA2	161	38.8/17	7.53/6.1	P07356	6 (15)
9	Heterogeneous nuclear ribonucleoprotein M/nucleic-acid binding	HNRPM	59	77.8/10.2	8.8/3.0	Q9E0D1	4 (5)
10	Keratin Kb40/intermediate filament organization	KRT78	91	86.1/8.0	8.66/7.8	Q6IFT3	3 (3)
11	Fab fragment of anti-VEGF antibody/angiogenesis	VEGF	195	23.5/5.0	6.35/8.7	1BJ1L	3 (23)
12	Peroxiredoxin-2/anti-oxidant activity	PRDX2	45	21.8/32	5.2/5.2	Q61171	3 (13)
13	Superoxide dismutase [Cu–Zn]/anti-oxidant activity	SOD1	65	15.9/20	6.03/6.9	P08228	3 (28)
14	Keratin, type II cytoskeletal 6A/intermediate filament organization	KRT6A	118	59.5/5.2	8.04/5.5	P50446	2 (3)
15	Stefin A3 protein/cysteine protease inhibitor	STFA3	92	11/17	6.28/6.3	Q497J0	10 (81)
16	Rpl30 protein/ribosome structure	RPL30	65	12.8/5.5	9.74/6.2	Q5PR1	1 (13)
17	[a]NID						
18-1	Calgranulin-B/calcium ion binding	S100A9	147	13.0/12	6.73/7.5	P31725	3 (24)
18-2	Calgranulin-B/calcium ion binding	S100A9	305	13.0/12	6.73/7.6	P31725	8 (46)
19	[a]NID						

Proteins with >2 fold changes (either increase or decrease) are included in this table. [a]NID = Not identified, [b]Mr — Theoretical/observed molecular weight in Daltons, and [c]pI— isoelectric point values were provided with the mass spectrometry data from The Centre for Genomic Application. Observed Mr and pI-values were estimated from the molecular weight marker run with each gel.

in specific compensatory changes in protein expression that can be assessed through proteomic analysis [19]. Recently, toxicoproteomics is being exploited for the discovery of biomarkers and organ specific toxicity/carcinogenicity signatures [20,21]. Here we used, proteomic analysis of mouse skin which offers a unique opportunity to study differentially expressed proteins following topical exposure. Short term topical exposure of DMBA is well reported to form DNA adducts in mouse skin [28]. About ~2600 protein spots were generated in mouse skin among control and different treatment groups. Among them, 22 differentially expressed proteins were exhibiting >2 fold change between treated and

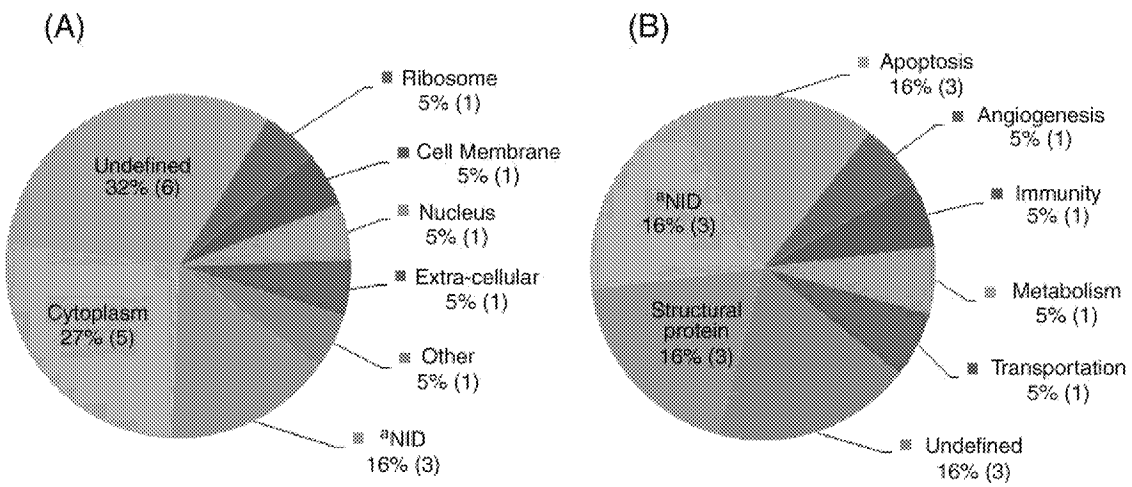

Fig. 3 – Pie charts showing distribution of the 22 identified proteins in mouse skin according to their (A) subcellular localization and (B) biological process on the basis of information through SWISS-PROT database. Numbers in parentheses are the values of differentially expressed proteins. [a]NID = Not identified.

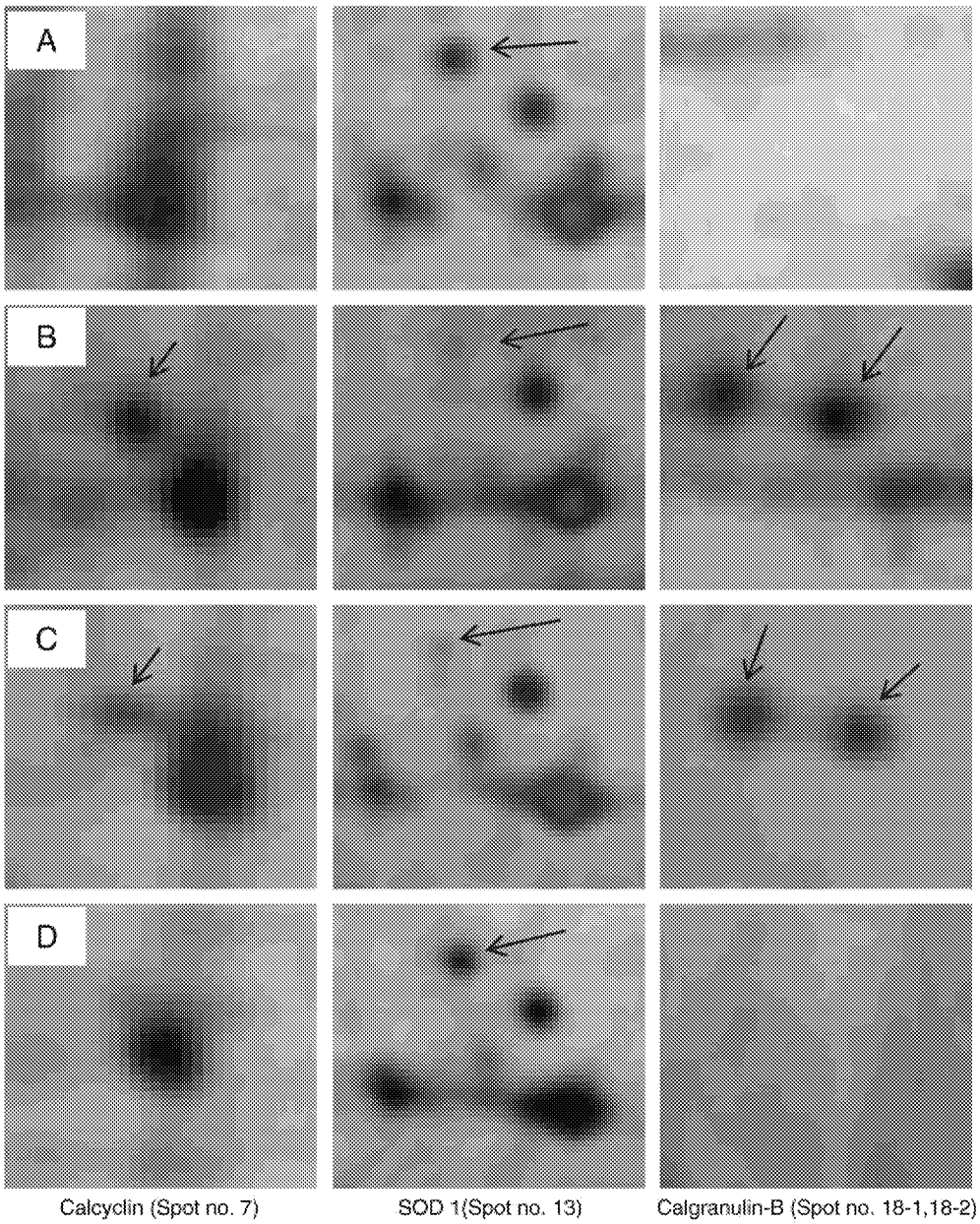

Fig. 4 – Zoomed images of 2-DE gel regions showing significantly ($p < 0.05$) up-regulated and down-regulated protein spots 7(calcyclin), 13(SOD 1), 18-1 and 18-2(calgranulin-B) of respective groups (A–D).

control tissues. Out of these, eEF1A1, CA III, annexin II, calcyclin, fab fragment of anti-VEGF antibody, PRX II, SOD 1, stefin A3 and calgranulin-B appeared to be of particular significance, as they were observed to be similar in terms of expression pattern in glyphosate and TPA-treated skin tissues (Fig 6).

The expression levels of eEF1A1, CA III and fab fragment of anti-VEGF antibody were markedly up-regulated following glyphosate and TPA treatment (Fig. 6). eEF1A1, the cofactor of eukaryotic protein synthesis is responsible for binding aminoacyl-tRNA to the ribosome during polypeptide elongation and its increased expression is directly proportionate to cellular proliferation [29], oncogenic transformation [30], apoptosis [31], and delayed cell senescence [32]. Increased amount of translation elongation factor-2 following exposure with TPA, a well known tumor promoter is reported [33]. CA III is a cytoplasmic enzyme known to play an important role in the cellular response to oxidative stress which in turn can mediate apoptosis [34]. Overexpression of CA III protects the cells from hydrogen peroxide-induced apoptosis [35]. Spot 11, identified as a fab fragment of anti-VEGF antibody is a breakdown fragment of VEGF, L-chain, and can be correlated

Fig. 5 – Peptide mass fingerprints of the mixture of tryptic peptides derived from (A) calcyclin, spot 7 and (B) calgranulin-B, spot 18-1 (C) SOD 1, spot 13. Details are given in Materials and methods section.

(A)

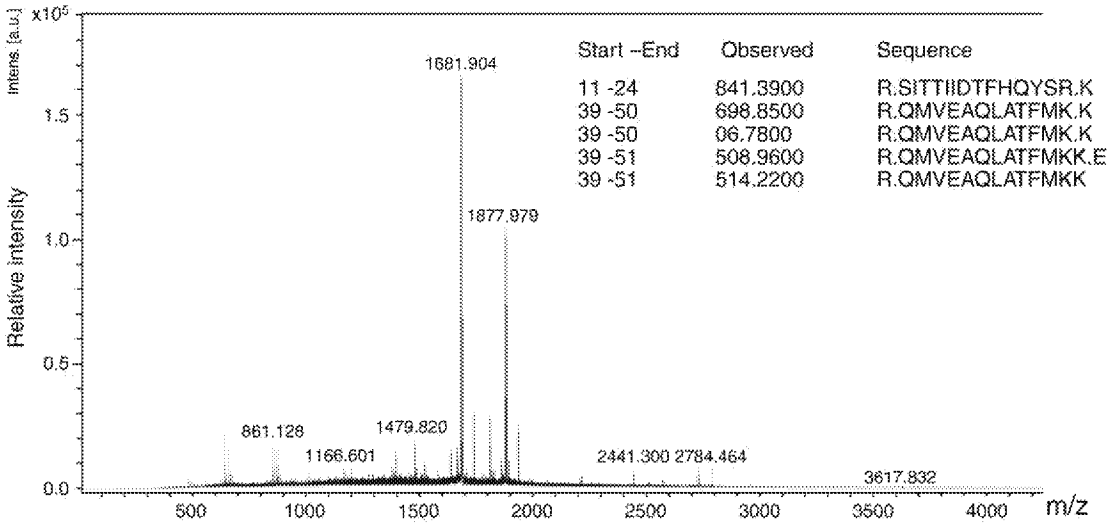

Start –End	Observed	Sequence
11 -24	841.3900	R.SITTIIDTFHQYSR.K
39 -50	698.8500	R.QMVEAQLATFMK.K
39 -50	06.7800	R.QMVEAQLATFMK.K
39 -51	508.9600	R.QMVEAQLATFMKK.E
39 -51	514.2200	R.QMVEAQLATFMKK

(B)

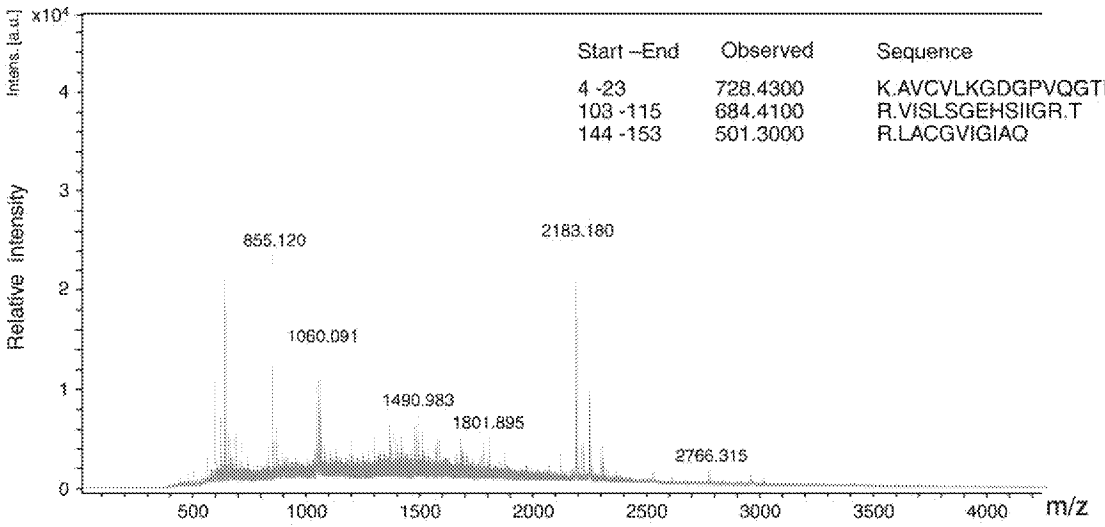

Start –End	Observed	Sequence
4 -23	728.4300	K.AVCVLKGDGPVQGTIHFEQK.A
103 -115	684.4100	R.VISLSGEHSIIGR.T
144 -153	501.3000	R.LACGVIGIAQ

(C)

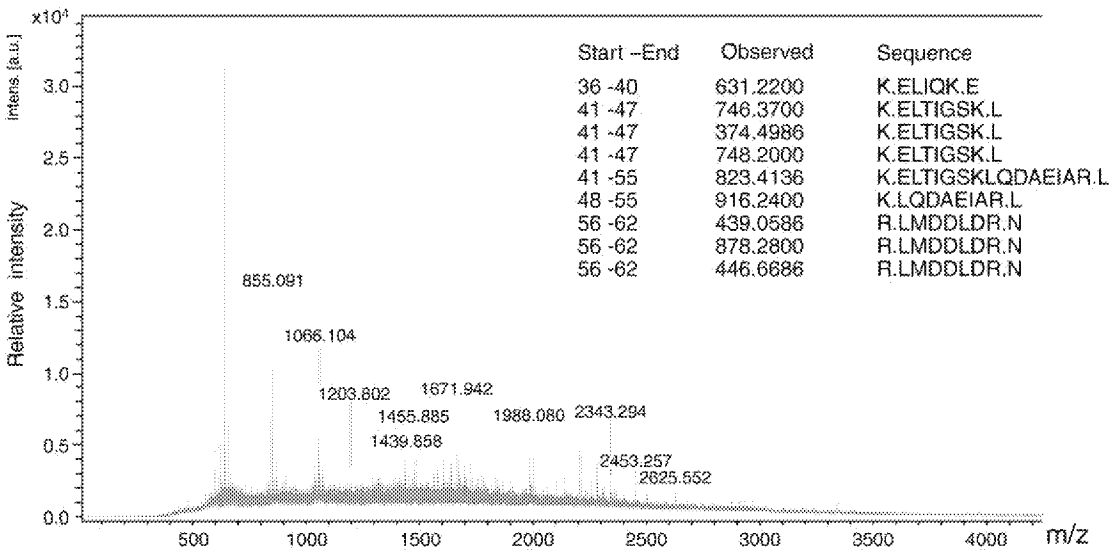

Start –End	Observed	Sequence
36 -40	631.2200	K.ELIQK.E
41 -47	746.3700	K.ELTIGSK.L
41 -47	374.4986	K.ELTIGSK.L
41 -47	748.2000	K.ELTIGSK.L
41 -55	823.4136	K.ELTIGSKLQDAEIAR.L
48 -55	916.2400	K.LQDAEIAR.L
56 -62	439.0586	R.LMDDLDR.N
56 -62	878.2800	R.LMDDLDR.N
56 -62	446.6686	R.LMDDLDR.N

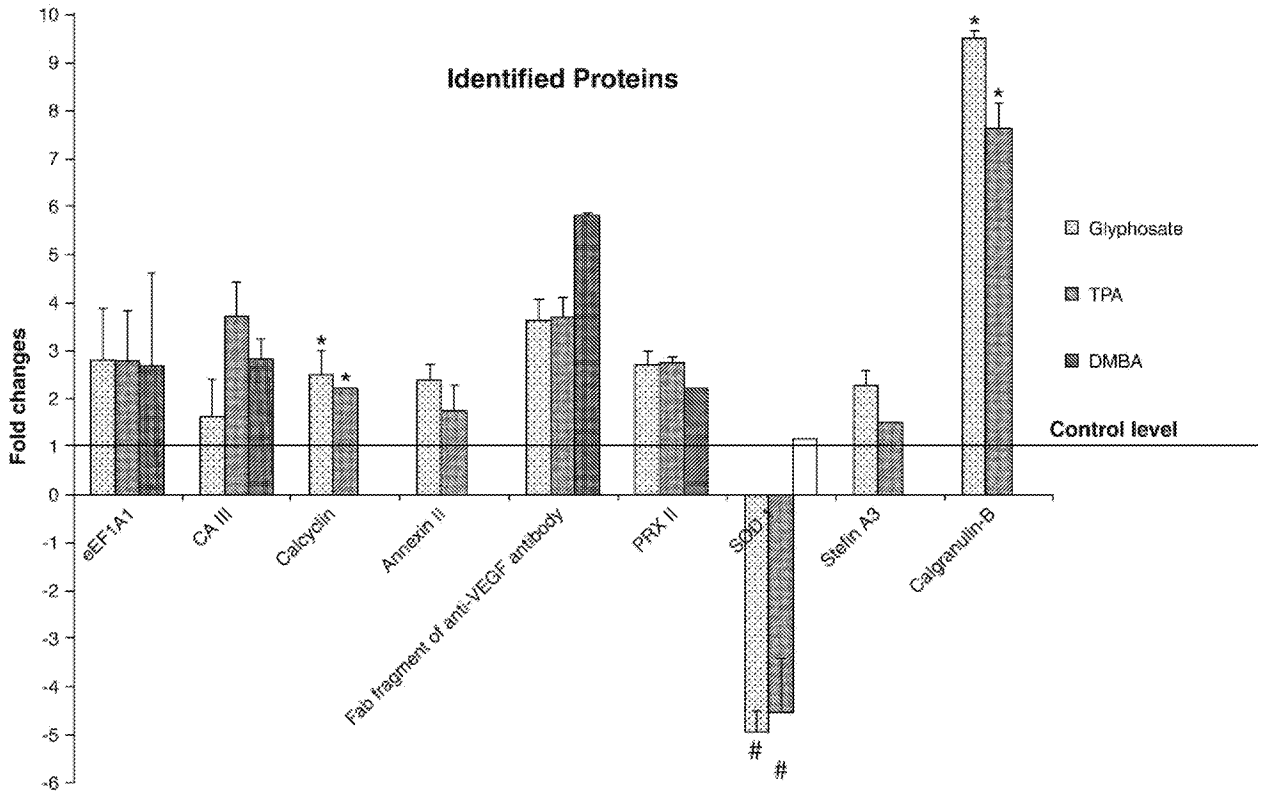

Fig. 6 – Changes in expression levels of the 9 different proteins that were affected by glyphosate, TPA and DMBA. Values are expressed as fold changes of the control or untreated values, indicated by the horizontal control level line. Values represent mean ± SD of 3 sets of experiments. *: Significantly up-regulated protein ($p < 0.05$). #: Significantly down-regulated protein ($p < 0.05$).

with the tumor promoting activity of test substances, as VEGF is a highly specific angiogenic factor that has been implicated in the angiogenesis, a prerequisite for neoplastic growth [36,37]. A number of studies have the role of angiogenesis in tumor growth [38,39].

Table 3 – Fold changes of differentially expressed proteins get altered by glyphosate, TPA and DMBA with respect to untreated group ($p < 0.05$).

Spot no.	Protein name	Fold changes		
		Glyphosate	TPA	DMBA
1	Translation elongation factor eEF-1 alpha chain (eEF1A1)	+2.80	+2.79	+2.67
3	Carbonic anhydrase III (CA III)	+1.62	+3.72	+2.81
7	Calcyclin	+2.48	+2.20	[a]n.d.
8	Annexin II	+2.38	+1.72	[a]n.d.
11	Fab fragment of anti-VEGF antibody	+3.64	+3.69	+5.80
12	Peroxiredoxin-2 (PRX II)	+2.73	+2.74	+2.20
13	Superoxide dismutase [Cu–Zn] (SOD 1)	−4.97	−4.56	+1.16
15	Stefin A3	+2.29	+1.49	[a]n.d.
18-1	Calgranulin-B	+9.52	+7.61	[a]n.d.
18-2	Calgranulin-B	+9.34	+7.43	[a]n.d.

Data represents mean ± SD of 3 experiments. (+) indicates up-regulation, whereas (−) indicates down-regulation by respective treatments. [a]n.d. indicates proteins that were not detected. For the clarity of the results here we mentioned calgranulin-B (18-2) separately but it is considered as a single protein.

Stefin A3 is known to play a role in skin growth and can be induced by TPA, leading to keratinocyte differentiation and proliferation [40,41]. Annexin II, a Ca^{2+} and phospholipid-binding protein is induced in various transformed cells and skin disorders [42–44]. Studies also showed up-regulated annexin II in a number of human cancers [45,46]. Thus up-regulation of annexin II by TPA and glyphosate is in consistency with its reported role in skin malignancies. PRX II, a novel group of peroxidases containing high anti-oxidant efficiency and which can also have a role in cell differentiation and apoptosis, was over-expressed in response to TPA, DMBA and glyphosate (Fig. 6, Table 3) [47]. PRX II not only protects the cells from oxidative damage caused by hydrogen peroxide, but can also endow cancer cells with resistance to both hydrogen peroxide and cisplatin towards radio-resistance [48]. Overexpression of PRX II in few cancers suggests that PRX has a proliferative effect and can induce cellular proliferation [49,50].

SOD1 provides a protective response against reactive oxygen intermediates and its over-expression level is accompanied by increased activity of anti-oxidant enzymes, namely, catalase, glutathione reductase, and glutathione. The suppression of skin carcinogen induced apoptosis, suggesting a combinatorial role in protecting skin cells from oxidative stress [51]. Thus down-regulation of SOD1, as observed in response to glyphosate and TPA exposure can potentiate process of tumor promotion (Fig. 6, Table 3).

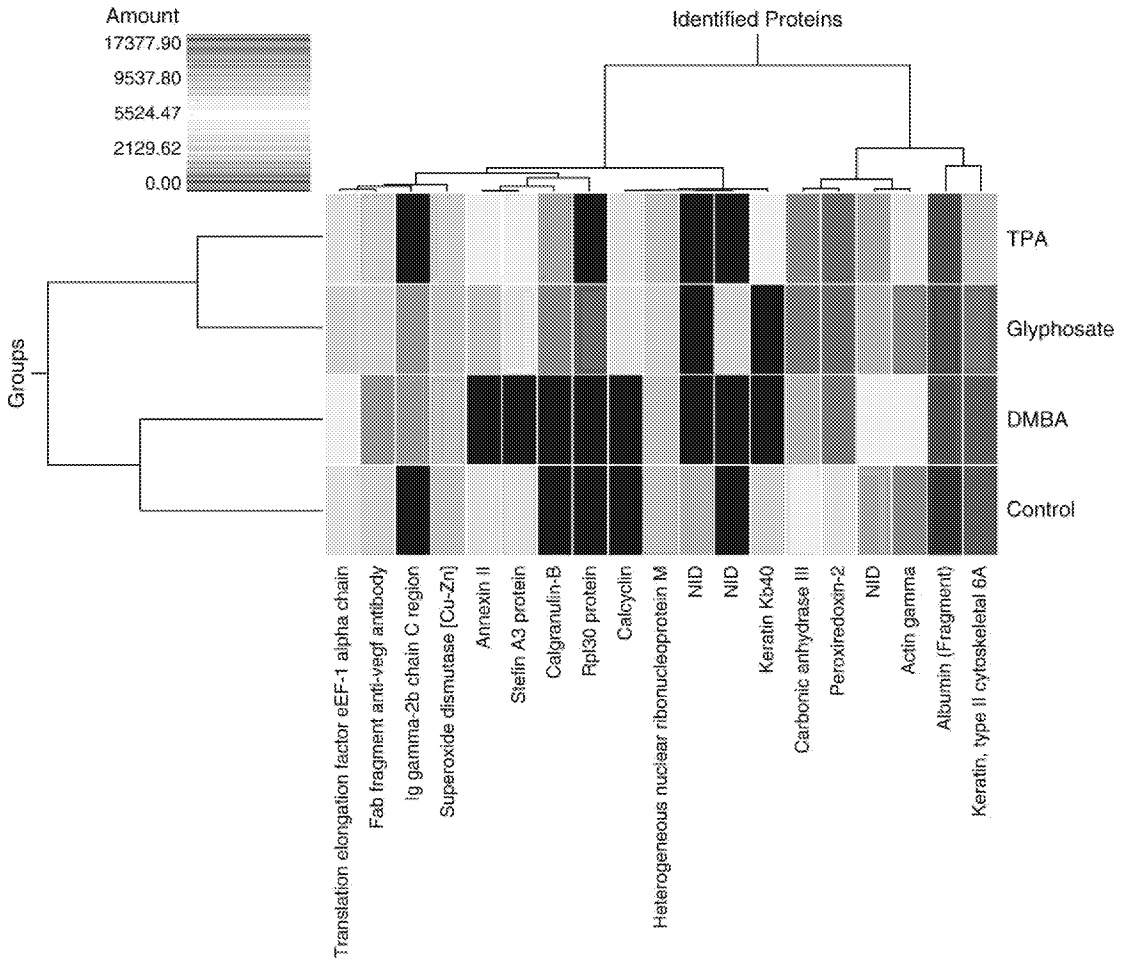

Fig. 7 – Two-dimensional hierarchical clustering map generated using identified protein expressions patterns induced by control, glyphosate, TPA and DMBA groups. Clusters were generated with normalized volumes of the differentially expressed protein spots. Each column represents an individual protein and each row represents an individual group.

Interestingly, S100A6 (calcyclin) and S100A9 (calgranulin-B) were expressed only in glyphosate and TPA-treated skin. These proteins are implicated in various key biological processes like cell cycle progression, differentiation, cancer development and metastasis [52]. Calcyclin, one of the two S100 proteins, was up-regulated by glyphosate (2.48-fold) and TPA (2.20-fold) in comparison to controls (Table 3). The S100A6 protein, in particular, is a well-established marker of melanoma cells in which its level correlates with tumor invasiveness and poor prognosis [53]. Several reports showed that S100A6 expression was increased in cancer [54,55]. Similarly, another protein calgranulin-B, was also up-regulated in the skin of glyphosate (9.52-fold) and TPA (7.61-fold) animals as compared to DMBA and untreated skin (Fig. 6, Table 3). In one of the studies, TPA is reported to induce calgranulin's S100A8 and S100A9 expression in mouse skin [56]. The induced expression of calcyclin and calgranulin-B by glyphosate and TPA was further confirmed by results of Western blotting.

Multivariate statistical analysis, such as hierarchical clustering, is one of the most popular methods to analyze large-scale gene expression data. There are few previous reports which have used this analysis for studying protein expression [22,57]. In this study, we applied 2-dimensional hierarchical clustering analysis to the changes of normalized significant differentially expressed protein spot volumes on respective 2-DE gels. This clustering analysis using 2-DE gel information also confirmed resemblance between tumor promoting activities of glyphosate and TPA. Thus this kind of multivariate statistical analysis using protein pattern expression may become widely applicable for primary screening of carcinogenicity for industrial and environmental pollutants.

Levels of the protein expression provide confirmatory evidence that expression of calcyclin, calgranulin-B and SOD 1 were altered by glyphosate and TPA treatment. Thus, from the reported studies and from our results, showing up-regulation of both calcyclin and calgranulin-B and down-regulation of SOD 1 by single exposure with TPA and glyphosate on mouse skin, it became clear that these proteins are involved in carcinogenesis and can be used as potential early biomarkers for skin carcinogenesis.

In summary, the 22 identified protein spots were expressed in mouse skin within 24 h following exposure to glyphosate, TPA and DMBA as proteomic signatures involved in

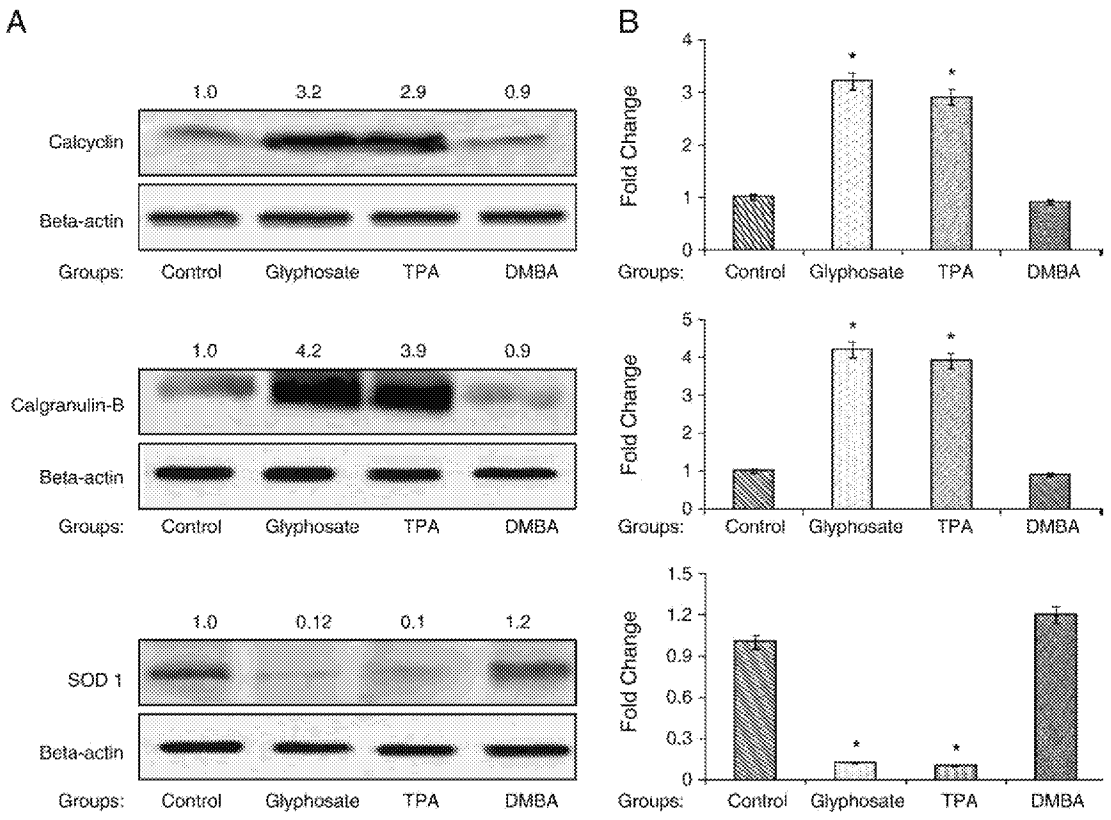

Fig. 8 – (A) Western blots showing expression of calcyclin, calgranulin-B and SOD 1 among control and treated groups. Equal loading of the samples was evaluated by reprobing the membranes with beta-actin antibody. * indicates significant difference, $p<0.05$. (B) Quantitative fold change, calculated with respect to control on the basis of pixel density measured by UNSCAN-IT software.

carcinogenic process. Out of these 22 proteins, 9 specific selected proteins are functionally related to apoptosis and growth-inhibition, anti-oxidation, energy metabolism, angiogenesis, calcium binding and protein biosynthesis processes with same expression profiles in glyphosate and TPA-treated animals. Among them, calcyclin, calgranulin-B and SOD 1 were identified to be closely associated with tumor promoting activity of glyphosate treatment therefore; their increased levels may be useful as biomarkers for tumor promotion. This study validates and consolidates the results of carcinogenicity data, showing that glyphosate has tumor promoting properties in mouse skin. In addition to providing an important framework, proteomic investigation serves as the starting point to develop a potential biomarker against pesticide induced carcinogenicity.

Acknowledgments

Authors are thankful to Director Lucknow, of Indian Institute of Toxicology Research, for his keen interest in the study. They would like to thank Ms. Babita Singh, Project Assistant, for her computer assistance in preparation of the manuscript. Authors are also thankful to TCGA, New Delhi for providing the MS analysis. The authors are grateful to Council of Scientific & Industrial Research, New Delhi, India for funding this work from Task Force project NWP-17.

REFERENCES

[1] Pimentel D. Pesticides and pest control, in: R. Peshin, A.K. Dhawan (Eds.), Integrated Pest Management: Innovation-Development Process, DOI 10.1007/978-1-4020-8992-3 3, Springer Science+Business Media B.V; 2009.
[2] United States Environmental Protection Agency (USEPA. Department of Environmental Protection. Washington, DC: Office of Pesticide Programs; 2002.
[3] International Agency for Research on Cancer (IARC. Monographs on the evaluation of carcinogenic risk to humans occupational exposures in insecticide application, and some pesticides. Lyon: IARC Press; 1991. 9.
[4] Williams GM, Kroes R, Munro IC. Safety evaluation and risk assessment of the herbicide Roundup and its active ingredient, glyphosate, for humans. Regul Toxicol Pharmacol 2000;31:117–65.
[5] Amrhein N, Deus B, Gehrke P, Steinrucken HC. The site of the inhibition of the Shikimate pathway by glyphosate: II. Interference of glyphosate with chorismate formation in vivo and in vitro. Plant Physiol 1980;66:830–4.
[6] Pieniazek D, Bukowska B, Duda W. Glyphosate—a non-toxic pesticide? Med Pr 2003;6:579–83.
[7] United States Environmental Protection Agency (USEPA) U.S. Environmental Protection Agency Reregistration Eligibility Decision (RED) Glyphosate. EPA-738-R-93-014. Washington, DC, 1993.
[8] De Roos AJ, Zahm SH, Cantor KP, Weisenburger DD, Holmes FF, Burmeister LF, et al. Integrative assessment of multiple

pesticides as risk factors for non-Hodgkin's lymphoma among men. Occup Environ Med 2003;60:E11.
[9] Hardell L, Eriksson M, Nordstrom M. Exposure to pesticides as risk factor for non Hodgkin's lymphoma and hairy cell leukemia: pooled analysis of two Swedish case-control studies. Leuk Lymphoma 2002;43:1043–9.
[10] Lin V, Garry V. In vitro studies of cellular and molecular development toxicity of adjuvants, herbicides, and fungicides commonly used in Red River Valley, Minnesota. J Toxicol Environ Health A 2000;60:423–39.
[11] Maibach HI. Irritation, sensitization, photoirradiation and photosensitization assay with a glyphosate herbicide. Contact Dermatitis 1986;15:152–6.
[12] Bolognesi C, Bonatti S, Degan P, Callerani E, Peluso M, Rabboni R, et al. Genotoxic activity of glyphosate and its technical formulation Roundup. J Agric Food Chem 1997;5:1957–62.
[13] Lioi MB, Scarfi MR, Santoro A, Barbieri R, Zeni O, Di Berardino D, et al. Genotoxicity and oxidative stress induced by pesticide exposure in bovine lymphocyte cultures in vitro. Mutat Res 1998;1–2:13–20.
[14] Lioi MB, Scarfi MR, Santoro A, Barbieri R, Zeni O, Salvemini F, et al. Cytogenetic damage and induction of pro-oxidant state in human lymphocytes exposed in vitro to gliphosate, vinclozolin, atrazine, and DPX-E9636. Environ Mol Mutagen 1998;1:39–46.
[15] Prasad S, Srivastava S, Singh M, Shukla Y. Clastogenic effects of glyphosate in bone marrow cells of Swiss albino mice. J. Tox. 2009, Article ID 308985, 6 pages, doi:10.1155/2009/308985.
[16] Moriya M, Ohta T, Watanabe K, Miyazawa T, Kato K, Shirasu Y. Further mutagenicity studies on pesticides in bacterial reversion assay systems. Mutat Res 1983;3–4:185–216.
[17] Palitti FC, Tanzarella R, Cozzi R, Ricondy E, Vitagliana A, Fiori M. Comparison of frequencies of SCEs induced by chemical mutagens in bone-marrow spleen and spermatogoneal cells of mice. Mutat Res 1982;2:191–5.
[18] Çelik M, Unal F, Yuuzbaşıoglu D, Ergun MA, Arslan O, Kasap R. In vitro effect of karathane LC (dinocap) on human lymphocytes. Mutagenesis 2004;2:101–4.
[19] Huang CM, Foster KW, De Silva T, Zhang J, Shi Z, Yusuf N, et al. Comparative proteomic profiling of murine skin. Invest Dermatol 2003;1:51–64.
[20] Wetmore BA, Merrick BA. Toxicoproteomics: proteomics applied to toxicology and pathology. Toxicol Pathol 2004;6:619–42.
[21] Anwar WA. Biomarkers of human exposure to pesticides. Environ Health Perspect 1997;4:801–6.
[22] Yamamoto T, Kikkawa R, Yamada H, Horii I. Investigation of proteomic biomarkers in in vivo hepatotoxicity study of rat liver: toxicity differentiation in hepatotoxicants. J Toxicol Sci 2006;1:49–60.
[23] Lynch D, Svoboda J, Putta S, Hofland HE, Chern WH, Hansen LA. Mouse skin models for carcinogenic hazard identification: utilities and challenges. Toxicol Pathol 2007;7:853–64.
[24] Shukla Y, Arora A, Singh A. Tumourigenic studies on deltamethrin in Swiss albino mice. Toxicology 2001;1:1–9.
[25] Rabilloud T, Vuillard L, Gilly C, Lawrence JJ. Silver-staining of proteins in polyacrylamide gels: a general overview. Cell Mol Biol (Noisyle-grand) 1994;40:57–75.
[26] Ramaswamy O, Guha-Mukherjee S, Sopory SK. Corelation of glyoxalase I activity with cell proliferation in *Datura* callus culture. Plant Cell Rep 1984;3:121–4.
[27] Marc J, Mulner-Lorillon M, Boulben S, Hureau D, Durand G, Belle R. Pesticide Roundup provokes cell division dysfunction at the level of CDK1/Cyclin B activation. Chem Res Toxicol 2002;15:326–31.
[28] Nigam N, Prasad S, Shukla Y. Preventive effects of lupeol on DMBA induced DNA alkylation damage in mouse skin. Food Chem Toxicol 2007;45:2331–5.
[29] Sanders J, Brandsma M, Janssen GMC, Dijk J, Moller W. Immunofluorescence studies of human fibroblasts demonstrate the presence of the complex of elongation factor-1bgd in the endoplasmic reticulum. J Cell Sci 1996;109:1113–7.
[30] Chi K, Jones DV, Frazier ML. Expression of an elongation factor 1 gamma-related sequence in adenocarcinomas of the colon. Gasteroenterology 1992;103:98–102.
[31] Chen E, Proestou G, Bourbeau D, Wang E. Rapid up-regulation of peptide elongation factor EF-1α protein levels in an immediate early event during oxidative stress-induced apoptosis. Exp Cell Res 2000;259:140–8.
[32] Shepherd JCW, Walldorf U, Hug P, Gehring WJ. Fruit flies with additional expression of the elongation factor EF1a live longer. Proc Nat Acad Sci USA 1989;86:7520–1.
[33] Gschwendt M, Kittstein W, Marks F. Effect of tumor promoting phorbol ester TPA on epidermal protein synthesis: stimulation of an elongation factor 2 phosphatase activity by TPA in vivo. Biochem Biophys Res Commun 1988;3:1129–35.
[34] Cotgreave A, Gredes R. Recent trends in glutathione biochemistry–glutathione–protein interactions: a molecular link between oxidative stress and cell proliferation? Biochem Biophys Res Commun 1998;242:1–9.
[35] Raisanen SR, Lehenkari P, Tasanen M, Rahkila P, Harkonen PL, Vaananen HK. Carbonic anhydrase III protects cells from hydrogen peroxide-induced apoptosis. FASEB J 1999;13:513–22.
[36] Dvorak HF, Brown LF, Detmar M, Dvorak AM. Vascular permeability factor/vascular endothelial growth factor, microvascular hyperpermeability and angiogenesis. Am J Pathol 1995;146:1029–39.
[37] Ferrara N. The role of vascular endothelial growth factor in pathological angiogenesis. Breast Cancer Res Treat 1995;36:127–37.
[38] Folkman J. Role of angiogenesis in tumor growth and metastasis. Semin Oncol 2002;6:15–8.
[39] Cavallaro U, Christofori G. Molecular mechanisms of tumor angiogenesis and tumor progression. J Neuro-oncol 2000; 1–2:63–70.
[40] Scott DK, Lord R, Muller HK, Malley RC, Woods GM. Proteomics identifies enhanced expression of stefin A in neonatal murine skin compared with adults: functional implications. Br J Dermatol 2007;6:1156–62.
[41] Dlugosz AA, Yuspa SH. Coordinate changes in gene expression which mark the spinous to granular cell transition in epidermis are regulated by protein kinase C. J Cell Biol 1993;120:217–25.
[42] Ozaki T, Sakiyama S. Molecular cloning of rat calpactin I heavy-chain cDNA whose expression is induced in v-src-transformed rat culture cell lines. Oncogene 1993;8:1707–10.
[43] Karimi-Busheri F, Marcoux Y, Tredget EE, Li L, Zheng J, Ghoreishi M, et al. Expression of a releasable form of annexin II by human keratinocytes. J Cell Biochem 2002;4:737–47.
[44] Bastian BC, van der Piepen U, Römisch J, Paques EP, Bröcker EB. Localization of annexins in normal and diseased human skin. J Dermatol Sci 1993;3:225–34.
[45] Vishwanatha JK, Chiang Y, Kumble KD, Hollingsworth MA, Pour PM. Enhanced expression of annexin II in human pancreatic carcinoma cells and primary pancreatic cancers. Carcinogenesis 1993;14:2575–9.
[46] Reeves SA, Chavez Kappel C, Davis R, Rosenblum M, Israel MA. Developmental regulation of annexin II (Lipocortin 2) in human brain and expression in high grade glioma. Cancer Res 1992;52:6871–6.
[47] Immenschuh S, Baumgart-Vogt E. Peroxiredoxins, oxidative stress, and cell proliferation. Antioxid Redox Signal 2005;5–6:768–77.
[48] Yo YD, Chung YM, Park JK, Ahn CM, Kim SK, Kim HJ. Synergistic effect of peroxiredoxin II antisense on cisplatin induced cell death. Exp Mol Med 2002;34:273–7.
[49] Kim K, Yu M, Han S, Oh I, Choi YJ, Kim S, et al. Expression of human peroxiredoxin isoforms in response to cervical carcinogenesis. Oncol Rep 2009;6:1391–6.

[50] Karihtala P, Mantyniemi A, Kang SW, Kinnula VL, Soini Y. Peroxiredoxins in breast carcinoma. Clin Cancer Res 2003;9:3418–24.
[51] Takahashi H, Hashimoto Y, Aoki N, Kinouchi M, Ishida-Yamamoto A, Iizuka H. Copper, zinc-superoxide dismutase protects from ultraviolet B-induced apoptosis of SV40-transformed human keratinocytes: the protection is associated with the increased levels of antioxidant enzymes. J Dermatol Sci 2000;23:12–21.
[52] Donato R. Functional roles of S100 proteins, calcium binding proteins of the EF-handtype. Biochim Biophys Acta 1999;1450:191–231.
[53] Weterman MA, Stoopen GM, van Muijen GN, Kuz´nicki J, Ruiter DJ, Bloemers HP. Expression of calcyclin in human melanoma cell lines correlates with metastatic behavior in nude mice. Cancer Res 1992;52:1291–6.
[54] Luo X, Sharff KA, Chen J, He TC, Luu HH. S100A6 expression and function in human osteosarcoma. Clin Orthop Relat Res 2008;466:2060–70.
[55] Fullen DR, Garrisi AJ, Sanders D, Thomas D. Expression of S100A6 protein in a broad spectrum of cutaneous tumors using tissue microarrays. J Cutan Pathol 2008;35:28–34.
[56] Gebhardt C, Breitenbach U, Tuckermann JP, Dittrich BT, Richter KH, Angel P. Calgranulins S100A8 and S100A9 are negatively regulated by glucocorticoids in a c-Fos-dependent manner and overexpressed throughout skin carcinogenesis. Oncogene 2002;21:4266–76.
[57] Wang X, Fan P, Song H, Chen X, Li X, Li Y. Comparative proteomic analysis of differentially expressed proteins in shoots of Salicornia europaea under different salinity. J Proteome Res 2009;7:3331–45.